Atmospheric Pollution Research 12 (2021) 125–135

Contents lists available at ScienceDirect

Atmospheric Pollution Research

journal homepage: www.elsevier.com/locate/apr

Temporal patterns of remote-sensed tropospheric carbon dioxide and methane over an urban site in Malawi, Southeast Africa: Implications for climate effects

Matthews Nyasulu [a,b,d], Md. Mozammel Haque [a,b,c,*], Kanike Raghavendra Kumar [e], Noel Banda [d], Brian Ayugi [f], Md. Jalal Uddin [g]

[a] Yale-NUIST Center on Atmospheric Environment, International Joint Laboratory on Climate and Environment Change (ILCEC), Nanjing University of Information Science & Technology, Nanjing, 210044, China
[b] School of Applied Meteorology, Nanjing University of Information Science and Technology, Nanjing, 210044, China
[c] Jiangsu Key Laboratory of Atmospheric Environment and Pollution Control, Jiangsu Collaborative Innovation Center of Atmospheric Environment and Equipment Technology, School of Environmental Science and Engineering, Nanjing University of Information Science & Technology, Nanjing, 210044, China
[d] Department of Climate Change and Meteorological Services (DCCMS)Malawi, P.O. Box 1808, Blantyre, Malawi
[e] Department of Physics, Koneru Lakshmaiah Education Foundation (KLEF), Vaddeswaram, 522 502, Guntur, Andhra Pradesh, India
[f] Key Laboratory of Meteorological Disaster, Ministry of Education (KLME)/Joint International Research Laboratory of Climate and Environment Change (ILCEC)/ Collaborative Innovation Center on Forecast and Evaluation of Meteorological Disasters (CIC-FEMD), Nanjing University of Information Science and Technology, Nanjing, 210044, China
[g] Collaborative Innovation Center on Forecast and Evaluation of Meteorological Disasters, School of Atmospheric Physics, Nanjing University of Information Science & Technology, Nanjing, 210044, China

ARTICLE INFO

Keywords:
Carbon dioxide
Methane
Biomass burning
Climatology
HYSPLIT
Malawi

ABSTRACT

Carbon dioxide (CO_2) and Methane (CH_4) are considered the most crucial climate forcing greenhouse gases due to their significant impacts on climate systems. The present study is aimed at analyzing the long-term (2004–2016) concentration patterns of CO_2 and CH_4 over Malawi located in Southeast Africa using the observations from Atmospheric Infrared Sounding (AIRS). The study found an annual increase concentration of CO_2 and CH_4, with a rate of 7.08% and 1.66%, respectively; whereas, the respective concentration levels of CO_2 and CH_4 in 2016 were noted as >400 ppm and >750 ppb, which is comparable to that reported by IPCC (2014) over the globe. The monthly and seasonal analyses revealed that high patterns are associated with biomass burning season, changes in vegetation cover, and long-range transport. The two trace gases were seasonally correlated with carbon-containing compounds produced from incomplete combustion and biomass burning. The trace gases and pollutants are emitted from the burning of crop residues during the harvesting season, besides, open burning of forests and vehicular emissions. The present study also detected a seasonal increase in CO_2 and CH_4 concentrations during JJA and SON seasons. The temperature (T °C) exhibited profound correlation with CO_2 ($r = 0.75$, $p < 0.01$) and CH_4 ($r = 0.80$, $p < 0.01$) during the pollution peak season of SON. Moreover, CO_2 and CH_4 showed significant positive correlation with cloud top temperature ($r = 0.56$, $p < 0.05$ and $r = 0.74$, $p < 0.01$, respectively) and negative correlation with cloud fraction ($r = -0.55$, $p < 0.05$ and $r = -0.69$, $p < 0.01$, respectively) during SON, imply extensive climatic effect by the trace gases during high pollution season. The backward air mass trajectories divulge a contribution of distant produced pollutants from neighboring Mozambique, Madagascar Islands, and the South American continent. The major sinks of tropospheric CO_2 and CH_4 observed from the present study are precipitation and vegetation.

Peer review under responsibility of Turkish National Committee for Air Pollution Research and Control.
* Corresponding author. Yale-NUIST Center on Atmospheric Environment, International Joint Laboratory on Climate and Environment Change (ILCEC), Nanjing University of Information Science & Technology, Nanjing, 210044, China.
E-mail address: mhaque@nuist.edu.cn (Md.M. Haque).

https://doi.org/10.1016/j.apr.2021.02.005
Received 28 September 2020; Received in revised form 18 January 2021; Accepted 5 February 2021
Available online 8 February 2021

1. Introduction

Carbon dioxide (CO_2) and Methane (CH_4) contribute 65% and 17%, respectively, of the total radiative forcing from the historical greenhouse gases (GHGs) (IPCC, 2014). These gases are both naturally and anthropogenically emitted into the atmosphere (Baeket al., 2014). Biomass burning is the main source of gaseous pollutants, including CO_2 and CH_4 (Crutzen, 1990). CO_2can be emitted into the atmosphere through biomass burning or land-use change and then sinks back to the land or oceans. CH_4 is mostly sourced from biomass burning, wetlands, agriculture, and waste, as well as oceanic and geological (Kirschke et al., 2013; Shi et al., 2015; Saunois et al., 2016). Most of the CH_4 is removed by the reaction with hydroxyl radicals (OH) initiated by pollutants such as NO_x, which then generates ozone in the troposphere (Kim et al., 2015; Saunois et al., 2016). They are also influenced by regional sources, long-distance transport, meteorology, economic development, as well as topography (Sreenivas et al., 2016a, 2016b; Ncipha et al., 2020; Wei et al., 2020). Even though trace gases can be removed from the atmosphere, recent studies show that the level of trace gases in the atmosphere, such as CO_2 and CH_4, has drastically increased from the pre-industrial level, with the current global level surpassing 400 ppm and 750 ppb, respectively (IPCC, 2014; WMO, 2019). This is signifying total emissions have surpassed the total sinks. Such an increase in atmospheric concentration poses a threat to the future climate, human health, and the environment (Lingaswamy et al., 2017).

From the past decades, significant effort has been made to monitor CO_2 and CH_4 in the atmosphere, providing detailed information about the distribution and trends of GHGs for climate studies at both global and regional scale (Keeling et al., 1976; Nakazawa et al., 1997; Tans et al., 1990; Brunke et al., 2009; Billett and Harvey, 2013; Lingaswamy et al., 2017; Machida et al., 2008). Even though such significant steps have been taken, it remains a challenge in most developing countries to have a continuous record of these gasses due to lack of skills as well as modern measuring equipment; as such long-term assessment of atmospheric GHGs and their associated impacts becomes uncertain. However, with the application of remote sensing technology specifically, satellite observations, which can provide continuous measurements of data in space and time, offers a better platform for continuous monitoring of these trace gases in the atmosphere and assess their impacts on the climate, human health, and environment (Wagner et al., 2008; Abed et al., 2017).

In recent years, Malawi has experienced changes in climate patterns such as floods, droughts, and temperature variations (Joshua et al., 2016). Several studies have been carried out to assess the driving factors of these changes in climatic patterns, such as those of (Nicholson et al., 2014) with less detailed the contribution of trace gases, e.g., CO_2 and CH_4, specifically in the lower atmosphere where most of the weather systems take place. Several studies in different environments have found the implication of these trace gases on local and regional climate (Ramanathan et al., 1985; Hansen et al., 2007; Yadav et al., 2017; Burney and Ramanathan, 2014; Deltedesco et al., 2019; Sparrevik et al., 2020). To the knowledge of the present study, there are no studies focused on the long-term patterns of trace gas concentrations in the atmosphere over Malawi. Therefore, it is worth and wealthy to consider monitoring and analyzing long-term atmospheric trace gases and their implication to the climate over Malawi, where climate change impacts are at an alarming rate. Regarding this, the present study analyses the patterns of tropospheric CO_2 and CH_4 concentrations over the urban site of southern Malawi using remotely sensed data sets retrieved from the Atmospheric Infrared Sounder (AIRS) onboard NASA's Aqua satellite. The study provides detailed temporal concentration patterns of the two important trace gases for the study period from 2004 to 2016.

The investigation of regional contribution to the concentrations of CO_2 and CH_4 is well examined. Further, we have also discussed the climatic effects of trace gases in the Southeast Africa region. The rest of the paper is structured as follows: section 2 outlines the study domain and local meteorology; section 3 details the data sets and approach to the present study. Results and discussions are given in section 4, while section 5 presents the main conclusions drawn from the current work.

2. Study domain and local meteorology

Malawi (Fig. 1) lies in the southeast part of the African continent. The country is stretched between latitudes 9°S-17°S and longitudes 32°E−36°E. To be specific, trace gas data was retrieved over Blantyre, an urban site of southern Malawi (15.78°S, 35.05°E). The topography of the surrounding areas of the sampling site is relatively low to the West and South while high to the East. It is characterized by high population density with major industries, as well as more traffic intensity (Mapoma et al., 2014). Based on the National Statistics Office Malawi 2018 (http://www.nsomalawi.mw/), the southern areas of Malawi have the highest population of about 7.751 million people with an estimated population density of about 2286 per square kilometer over the urban area. The basic climatic features of the study area are presented in Fig. 2. The meteorological variables observed at Chichiri Meteorological station in the city of Blantyre showed high temperatures (Fig. 2a) between September and November but gradually decreased with the lowest recorded in July. Conversely, the wet months (Fig. 2b–c) start from October with the maximum precipitation recorded in January and ends in March; the rest of the season is dry. Interestingly, the dry season (May–October) coincides with the active fire hotspots, as shown in Fig. S1 of Supplementary Material (SM). The seasonal wind pattern over the study domain and surrounding region depicts a convergency system of south easterly and north easterly air mass as Inter-Tropical Convergence Zone (ITCZ) during the wet months of December to February, and south easterlies from March to August (Fig. S2). Meanwhile, strong easterlies dominate during the September–November (SON) period.

The study domain lies in a region of active biomass burning, including indoor biomass burning of wood/charcoal for energy, burning of crop residues by farmers during post-growing as well as pre-growing season to clear the fields (Vakkari et al., 2018). Moreover, it is also characterized by open burning, such as man-made forest fires, particularly during the dry season (Queface et al., 2003; Robles, 2008; Adesina et al., 2015; Nyasulu et al., 2020). In a bid to understand the impact of biomass burning over the region, the study utilized the data from the Moderate Resolution Imaging Spectroradiometer (MODIS) sensor observed on the selected days of each which were consistent for each month of the year 2016 as a representative for the examination of fire hotspots over the study domain. The spatial patterns show that the fire hotspots advance from May to October, indicating a high rate of open burning (Fig. S1) over the study domain.

3. Data and methods

CO_2 and CH_4 datasets used in this study were retrieved from the Atmospheric Infrared Sounding (AIRS). The AIRS is a hyper spectral sensor flown aboard the National Aeronautics and Space Administration (NASA) Aqua satellite (Chahine et al., 2005, 2008). It has 2378 spectral channels within 0.41–15.4 μm that can measure several trace greenhouse gases in the troposphere, including CO_2 and CH_4. It passes over the equator at approximately 1:30 a.m. and 1:30 P.M that result in global coverage twice a day. The validation of CH_4 using in situ aircraft observation has proven that the bias of the retrievals is approximate −1.4%–0.1%, and the root mean square is about 0.5%–1.6% (Xiong et al., 2008). The estimates of CO_2 from AIRS agree to the approximate of about ±0.5% in the mid-troposphere between the latitudes ±65° with NOAA ESRL/GMD aircraft data retrievals (Maddy et al., 2008). The present study utilized tropospheric mole fractions of CO_2 and CH_4 level 3 version 5 products for the period 2004–2016 at a spatial resolution of 2.5 ° × 2.5 ° and 1 ° × 1 °, respectively. To construct a long-term monthly time series, the present study averaged the monthly values at a grid box corresponding to the resolution of the data at the selected site.

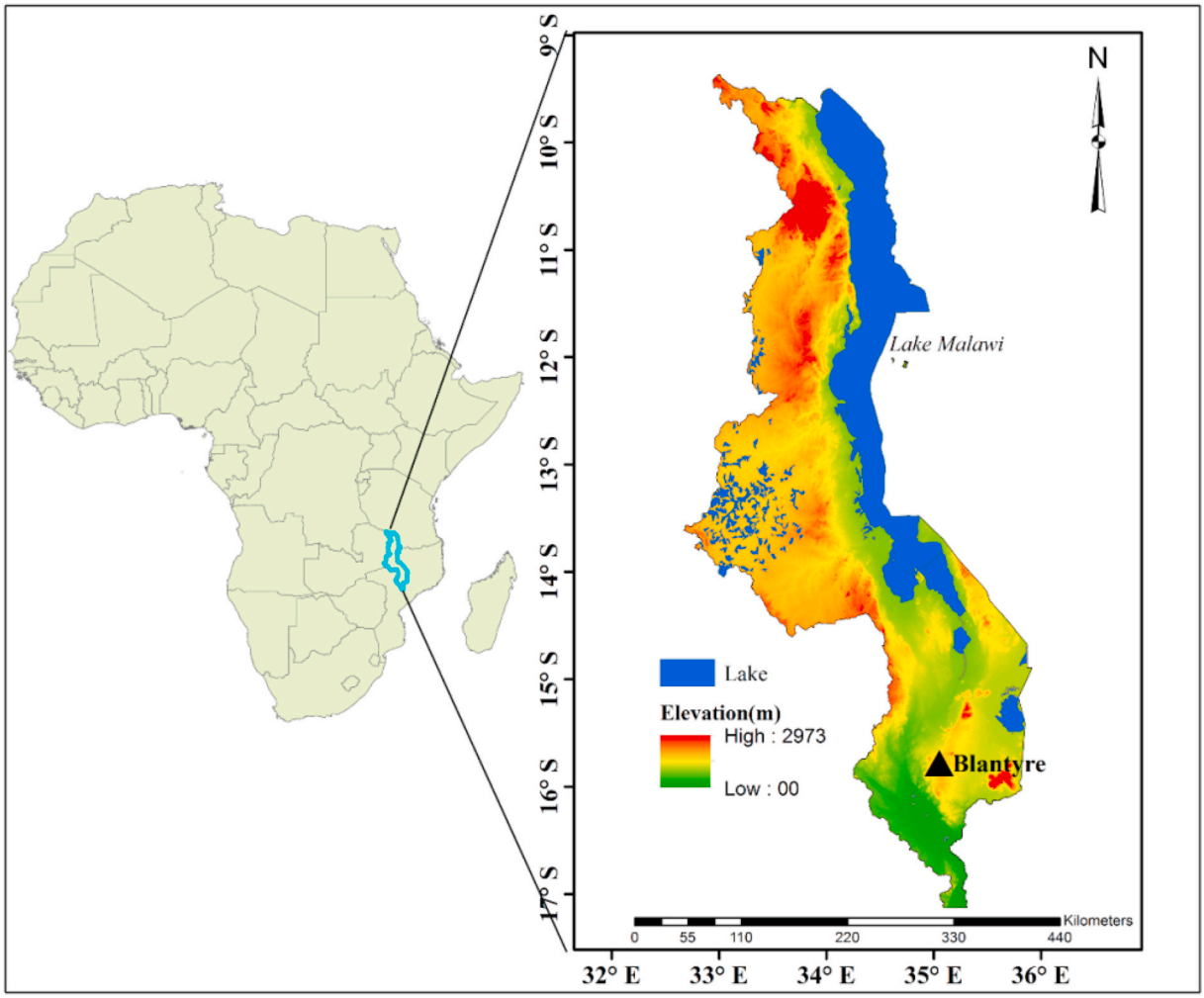

Fig. 1. Location and topographic map of Malawi. The black triangle show the site data sets were observed.

The average area technique is provided by GES DISC through a web-based application known as Giovanni. The NASA data and more information about the download technique are available on https://giovanni.gsfc.nasa.gov/giovanni/. More details on data retrievals and validation have been documented by several authors and hence not repeated here to avoid duplication (Chahine et al., 2005, 2008; Maddy et al., 2008; Engelen et al., 2009; Strow et al., 2008; Rajab et al., 2012; Kahn et al., 2014; Xiong et al., 2008; Cao et al., 2019). In the past decade, AIRS retrieved CO_2 and CH_4 have been widely used in atmospheric research studies in different environments (Bai et al., 2010; Singh et al., 2015; Abed et al., 2017). The significance of utilizing AIRS is that it can provide trace gases even during cloudy conditions without the use of information from the models. As such, the present study had no missing data for the entire study duration.

To determine the variations of meteorological variables, the present study utilized the key parameters, namely; temperature, relative humidity, and precipitation. The daily variables were observed at Chichiri Meteorological station with the latitude 15.78 °S and longitude 35.05 °E. All the meteorological parameters were sourced from the local weather agency, the Department of Climate Change and Meteorological Services Malawi for the entire study period. The daily variables were averaged to create a long-term climatology of the selected site. The pollutants were retrieved in the surface to compare whether the local emissions contributed to the variation of tropospheric trace gases. Furthermore, the study analyzed the influence of the Vegetation Index on the concentration of CO_2 and CH_4 for the entire study period. Pollutants and Vegetation Index data were retrieved in the same period as CO_2 and CH_4, were all obtained from the NASA's Earth Observation data available at https://earthdata.nasa.gov/. The retrieving method, similar to CO_2 and CH_4, was also employed for the pollutants and Vegetation Index data. Furthermore, the study used thermal radiance data to show evidence of active open biomass burning over the study domain. The MODIS collection 6.1 was employed in the current study, with more details on the datasets is available at https://firms.modaps.eosdis.nasa.gov/.

In this study, four major meteorological seasons were considered, namely: December-January-February (DJF), March-April-May (MAM), June-July-August (JJA), and September-October-November (SON). To evaluate the seasonal changes during the study period, the research employed linear regression analysis. However, linear regression could not detect abrupt changes in the time series. Therefore, the study further applied the Mann-Kendall (MK) sequential test to detect such changes in the CO_2 and CH_4 concentrations (Mann, 1945; Kendall, 1975). The study also considered the statistic introduced by Sneyers (1990). These include forward statistic $u'(t)$ and backward sequential statistic $u(t)$. The subsequent forward statistic is a standardized variable with a unit standard deviation and zero means. These statistics were computed using the MK test for each season during the whole study period. The confidence limit of the standard normal Z values is at a = 5%. The upper and lower confidence limits correspond to ±1.96. When the progressive MK values exceed confidence limit points, it signifies a significant trend at a 5% significance level. The above approach is useful in both short-term and long-term climatic studies and has recently been used by many researchers (Ayugi et al., 2018; Chatterjee et al., 2014; Zarenistanak et al.,

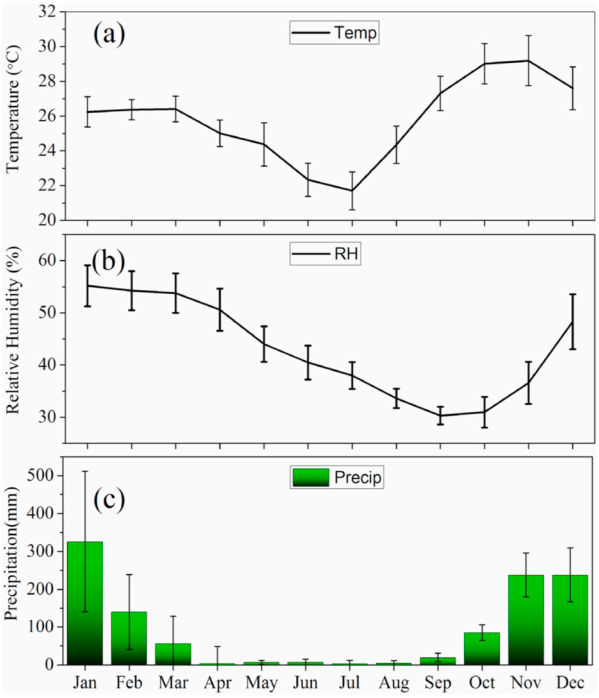

Fig. 2. Monthly variations of averaged meteorological variables (a) Temperature, (b) Relative humidity and (c) precipitation observed over Blantyre during 2004–2016.

2020).

The changes in vegetation and water vapor can contribute to both increases and decrease the concentration of trace gases in the atmosphere. The burning of vegetation results in the emission of pollutants into the atmosphere or, in the other way, absorbs pollutants such as CO_2 for photosynthetic processes. In this study, we have employed the Normalized Difference Vegetation Index (NDVI) from the MODIS-Terra platform at a spatial resolution of 0.5° to understand its relationship. The NDVI is defined as the ratio of albedo (α) observed at different wavelengths:

$$NDVI = \frac{\alpha_{0.86\mu m} + \alpha_{0.67\mu m}}{\alpha_{0.86\mu m} - \alpha_{0.67\mu m}} \quad (1)$$

where 0.86 μm and 0.67 μm are for NIR and red, respectively. The values can vary between −0.1 and 1.0 though the common values are between 0.1 and 0.7. The higher NDVI, the greater the density and greenness of plant canopies (Sreenivas et al., 2016a, 2016b). Furthermore, the study compared with the level 3 water vapor obtained from AIRS at a resolution of 1° with the trace gases for the entire study period to deduce whether the variation of the two variables influenced each other. Water vapor and photolysis of ozone (O_3) are the primary sources of hydroxyl (OH) radicals (Eisele et al., 1997; Sreenivas et al., 2016a, 2016b). OH are the most reactive and responsible for the oxidation of all gasses in the atmosphere (Kim et al., 2015). The primary source can be defined as:

$$O_3 + h\nu(\leq 310nm) \rightarrow O_2 + O(\varnothing) \quad (2)$$

where $O(\varnothing)$ is the electronically excited atom.

$$O(\varnothing) + O_2 \rightarrow O + M \quad (3)$$

$$O(\varnothing) + H_2O \rightarrow 2OH \quad (4)$$

In the atmosphere, pollutants such as NO_x can initiate the reaction between OH radicals and trace gases. For example;

$$HO_2 + NO \rightarrow OH + NO_2 \quad (5)$$

$$CH_4 + OH \rightarrow CH_3 + H_2O \quad (6)$$

It is through equation (6) where most of the pollutants like CH_4 are washed out from the atmosphere.

In the interest of understanding the contribution of long-distance sources of pollutants, the study used the HYSPLIT model (Draxler and Hess, 1997) to analyze air mass pathways reaching the study domain. A 5-day backward air mass trajectory arriving at a minimum altitude of 500 m above the ground level ending at the selected site was considered for the entire study duration, while the maximum altitude was set at 10, 000 m. All the air mass trajectories were computed using the HYSPLIT model-based Trajstat software (Wang et al., 2009).

4. Results and discussion

4.1. Monthly and seasonal variations

Fig. 3 shows the monthly mean changes of mid-tropospheric CO_2 and CH_4 concentrations observed from the AIRS during the study period. The results showed two peaks in the concentration of CO_2 pattern were recorded in July and December and drastically decreased in January, while the lowest was observed in April. It can also be noted from Fig. 3 that the peaks of CO_2 and CH_4 concentration do not coincide; signifying different factors influence the tropospheric concentration of the two trace gases over the selected site. The averaged values of CO_2 were found to be 389 ppm and 388 ppm in December and July, respectively, during 2004–2016, while in April, it was 386 ppm. In contrast, CH_4 was recorded the highest in September and decreased to the lowest in January. The average of 1833 ppb was observed in September for the study period, while January marked with 1788 ppb. Seasonal averages showed high concentration of CO_2 during JJA and SON as well as low during MAM (Fig. S3). In contrast, CH_4 concentration was observed high during SON and low during DJF season (Fig. S3). It is observed that the variations of CO_2 and CH_4 concentration are highly associated with the changes in meteorological variables and anthropogenic activities. The key meteorological variables such as air temperatures, relative humidity, and rainfall decrease from April over the site, and generally, the weather is cold until July (Fig. 2). To sustain the cold weather, there is an increasing scenario of indoor biomass burning, such as the increased usage of wood-burning is observed in Malawi to get warmth against cold winters. Moreover, it is also the end of the crop growing season, where most of the farmers burn the agricultural waste (crop) residues from May (dry period). Such activities enhance the concentration of trace gases in the troposphere.

Also, the regional open biomass burning, such as man-made bush fires, largely contributed to the concentration pattern of CO_2 and CH_4.

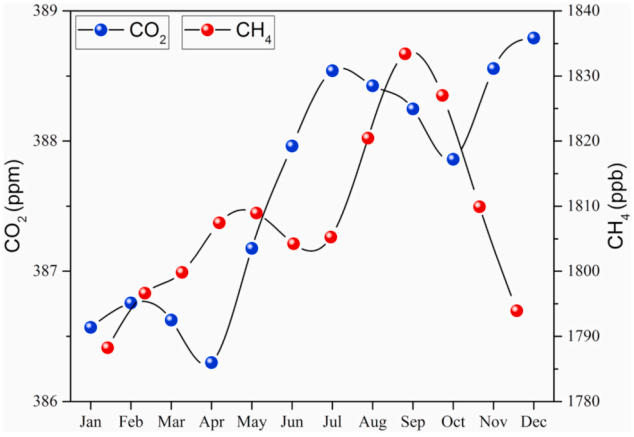

Fig. 3. Monthly average concentration of CO_2 and CH_4 during the entire study period.

This is supported by Fig. S1 where the density of fire hotspots obtained from the MODIS due to burning gradually increase from May to October, as the two gases were observed to be relatively high. Besides, vehicle and industrial emissions also produce a large number of pollutants such as carbon monoxide (CO) along with CO_2 and CH_4 (Mapoma et al., 2014), which is widely spread by the strong winds (Nyasulu et al., 2020) results in the increased concentration levels. Furthermore, changes in tropospheric circulation accompanied by distant travel air mass played a key role in an increase of CO_2 level in the troposphere from April to July. More details about air mass are highlighted in section 4.7.

During June and July air masses in the lower troposphere mostly originated from the Indian Ocean, locally known as *Chiperoni weather* (Ngongondo et al., 2011; Fiwa et al., 2014), reduce the concentration levels of pollutants on the surface that results into the decrease of CH_4, on the other way CO_2 does not decrease, which is discussed in section 4.7. However, it is wealthy to emphasize that the level of OH radicals during this period is low; therefore, the impact on CH_4 sinking is lower than that observed during the wet season. A decrease in CH_4 from November is due to the reduced anthropogenic activities accompanied by the onset of the rains, which are associated with an increase of OH radicals that reacts with CH_4. Further, December is observed to be influenced by north easterly air mass (see Fig. 9 and section 4.7) through northeasterly trade winds (Fig. S2). Such air mass carries the pollutants from polluted regions of the Middle East, increasing of CO_2 level in December. However, as the peak of rainfall approaches (December–February), there is a drastic decrease in CO_2 because of convective processes that bring heavy rain, which washes out CO_2. Moreover, less anthropogenic activities, and regeneration of vegetation cover that absorbs CO_2, reduced the level of CO_2 during the subsequent months.

4.2. Inter-annual patterns

The present study found that the concentration of CO_2 and CH_4 in the troposphere increased by 7.08% and 1.66%, respectively, from 2004 to 2016. By 2016, an annual average of CO_2 was just above 400 ppm, while CH_4 was higher than 1809 ppb (Fig. 4). The results show that concentrations of CO_2 and CH_4 were increased gradually for the period 2004–2016. The above results revealed that the levels of emissions surpassed the levels of sinking, which could be attributed to increased anthropogenic activities such as excessive deforestation and biomass burning. CO_2 increased at a steady rate, with an average of 0.5% annually, while 0.1% for CH_4 was added into the troposphere annually. Going into specific years, a notable decrease of CH_4 was observed in 2006 and 2009 by 0.04% and 2013 by 0.18%. Considering the seasonal changes, Table 1 shows that CO_2 increased to >400 ppm in 2016, with the highest values noted in JJA (401 ± 0.87 ppm) and SON (402 ± 0.31 ppm). Similarly, CH_4 exhibited relatively higher values during SON and JJA compared to other seasons. Both gases were the most abundant during the dry seasons.

The trend from linear regression analysis for each season depicts a rapid increase in tropospheric CO_2 concentration at an average of 2.1 ppm per year. The trends for the respective seasons were 2.12, 2.24, 2.16, and 2.15 ppm per year for DJF, MAM, JJA, and SON. For CH_4, the dry seasons (JJA and SON) have a high contribution with 3.26 and 3.23 ppb for JJA and SON respectively each year, while DJF and MAM contributed to 1.69 and 2.45 ppb, respectively. The p-values for CO_2 and CH_4 were <0.05 signifying a significant increase of two trace gases. The Sequential Mann-Kendal test is shown in Fig. 5 and Fig. 6, revealed abrupt changes in 2010 for all the seasons, except CH_4 during the DJF season, while a significant change occurred in 2013. A notable decrease in CH_4 was observed between 2006 and 2007 during DJF, MAM, and JJA, which agrees with the inter-annual changes. The same could be associated with heavy rains over the region during these years (Kumbuyo et al., 2014; Alexander, 2017), resulted in a rapid sink of CH_4.

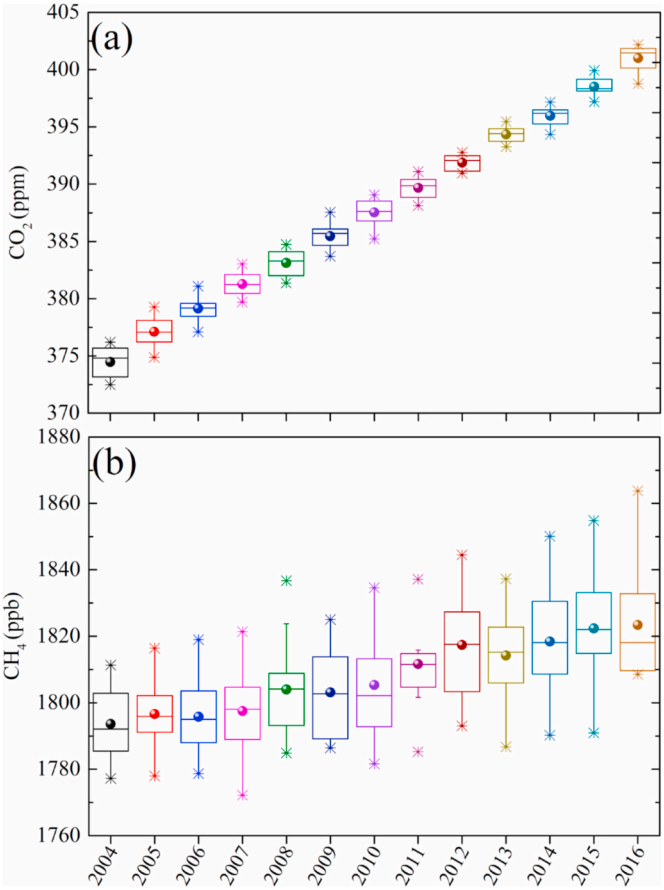

Fig. 4. Inter-annual variations of (a) CO_2 and (b) CH_4 from 2004 to 2016 in Blantyre, Malawi.

Table 1
Seasonal variations of CO_2 (ppm) and CH_4 (ppb) during the study period.

Year	DJF		MAM		JJA		SON	
	Mean	Std	Mean	Std	Mean	Std	Mean	Std
CO_2								
2004	374	1.87	373	0.59	375	0.53	376	0.49
2005	377	2.28	376	0.50	377	0.44	378	0.73
2006	379	1.45	378	0.76	380	0.84	379	0.32
2007	381	1.49	380	0.44	382	0.34	382	0.58
2008	383	1.19	382	0.38	384	0.31	384	0.90
2009	386	1.62	384	0.49	386	0.63	386	0.29
2010	387	1.71	387	0.63	389	0.56	388	0.68
2011	389	0.81	389	0.56	390	0.65	391	0.46
2012	392	0.76	391	0.32	392	0.33	393	0.30
2013	394	0.65	394	0.33	395	0.31	395	0.24
2014	395	1.08	395	0.62	397	0.21	396	0.64
2015	398	0.95	398	0.65	399	0.89	399	0.98
2016	400	1.27	401	0.90	401	0.87	402	0.31
CH_4								
2004	1786	12.97	1791	2.29	1793	10.87	1804	10.35
2005	1789	12.95	1796	3.65	1795	5.37	1806	10.51
2006	1785	6.85	1790	8.83	1800	7.03	1808	10.16
2007	1782	11.50	1799	4.40	1794	9.08	1815	8.68
2008	1793	11.72	1802	2.00	1799	8.84	1822	15.73
2009	1788	2.63	1801	12.3	1806	9.75	1817	10.63
2010	1788	5.35	1802	9.89	1806	7.26	1826	11.22
2011	1797	9.79	1812	2.03	1818	10.76	1830	15.60
2012	1796	2.90	1814	5.15	1824	9.94	1836	14.00
2013	1794	7.11	1815	3.58	1818	8.54	1830	11.40
2014	1797	11.05	1818	9.86	1822	10.67	1837	11.44
2015	1802	16.04	1820	6.81	1829	13.56	1839	16.92
2016	1810	0.97	1812	5.11	1828	10.99	1843	21.39

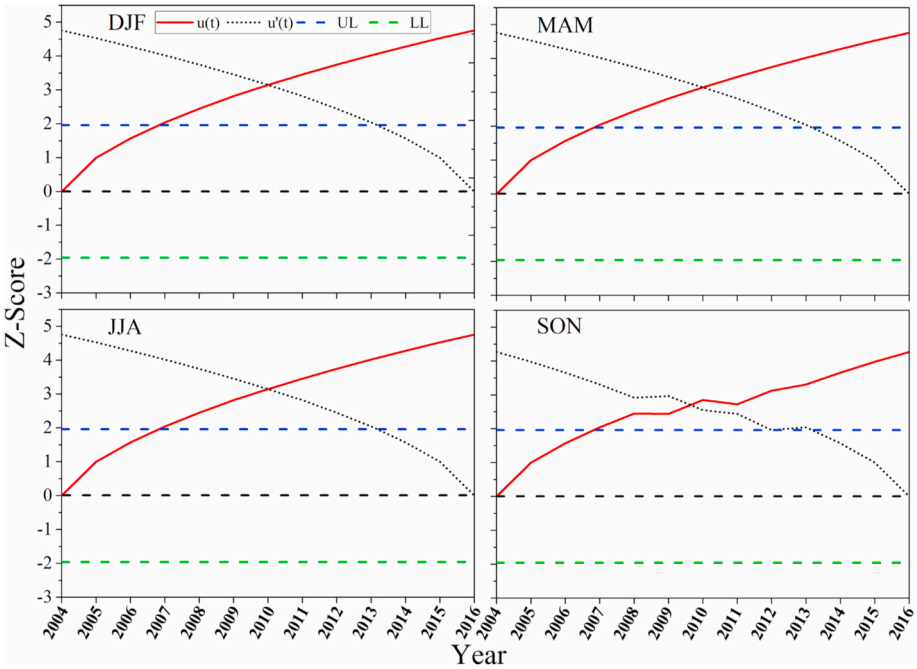

Fig. 5. Abrupt change in seasonal CO_2 derived from Sequential Mann-Kendal test statistic.

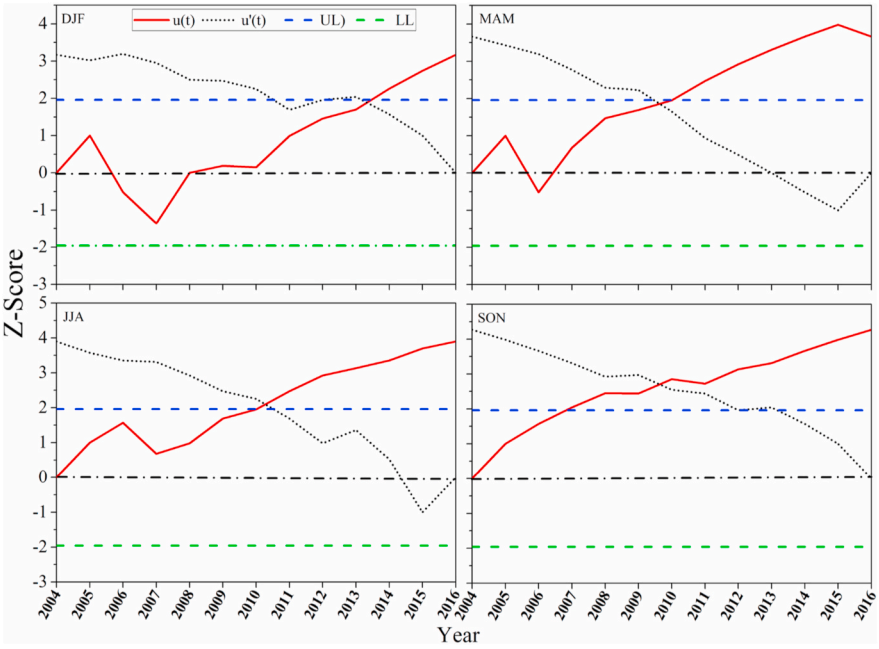

Fig. 6. Abrupt change in seasonal CH_4 derived from Sequential Mann-Kendal test statistic.

4.3. *Relationship of CO_2 and CH_4 with other pollutants*

CO_2 and CH_4 were compared with the carbon-containing compounds produced from the incomplete combustion, namely black carbon (BC), carbon monoxide (CO), and sulfur dioxide (SO_2) attributed from open biomass burning such as crop residues as well as coal combustion from industries and vehicle emissions (Mapoma et al., 2014). The results revealed an increase of the pollutants corresponds to the rise of these two trace gases, particularly CH_4, during the peak season of biomass burning (Fig. 7). This tells that the greenhouse gases, particularly CH_4, were emitted from the same source as the pollutants during the dry season from biomass burning. This is also supported by the correlation analysis between the pollutants and trace gases where positive correlations dominated. The correlations of CO_2 with BC, CO and SO_2 were 0.49 (P = 0.11), 0.42 (P = 0.18), and 0.14 (P = 0.14), respectively, indicating no significant relations among them. On the contrary, the correlations of CH_4 with BC, CO, and SO_2 were 0.87, 0.79, and 0.89, respectively, with P-value <0.01 suggesting a significant relationship between CH_4 and pollutants. Interestingly, the peaks of pollutants coincided with CH_4 as well as the correlations were stronger for CH_4 than CO_2. This implies that the concentration of CH_4 was much influenced by local sources as well as the surrounding region, while CO_2 was influenced by distant sources through long range air mass travel. More details about air masses are highlighted in section 4.7.

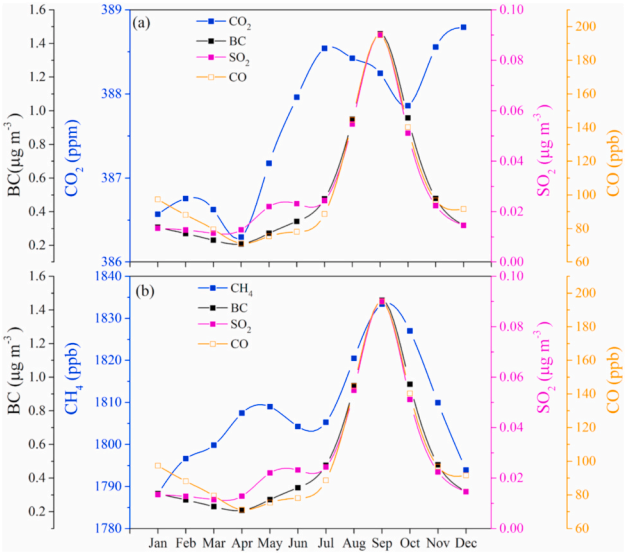

Fig. 7. Monthly variations of (a) CO_2 and (b) CH_4 with other pollutants of black carbon (BC), sulfur dioxide (SO_2), and carbon monoxide (CO).

4.4. Relationship of CO_2 and CH_4 with vegetation cover

We observed from the present study that CO_2 and CH_4 concentrations varied inversely with NDVI, except in December when CO_2 increased with the increment of NDVI (Fig. S5). Generally, the wet season starts in October (Fig. 2b–c) over the study domain, resulting in the regeneration of vegetation, consequently leading to a decrease in tropospheric CO_2. This is because the sprouting vegetation takes up most of the CO_2. However, most of the farmers excessively burn their fields to clear land for the growing season around November and December resulted in an increase of atmospheric CO_2 concentration in December. Further, CO_2 is enhanced by distant sources through changes in atmospheric circulation during December. And then, the CO_2 decreased in January due to the enhancement of vegetation cover when CO_2 was uptake by vegetation during the photosynthesis process. A slight increase in CO_2 during February could be due to the convergence system that brings up fresh pollutants such as CO from regions of active biomass burning. This, coupled with those locally produced that reacts with excessive OH to form CO_2. Nevertheless, the concentration of CO_2, along with other pollutants, dramatically decreased in April, probably due to less anthropogenic activities and changes in atmospheric circulations that inhibit the concentration of pollutants.

It is of interest to note that CH_4 concentration was found high in April than CO_2 attributed to different sources (e.g., wetlands) rather than anthropogenic emissions and the decrease of monthly rainfall. April is the cessation period of the rains in the southern areas of Malawi (Fig. 2). Compared to January, excess rains wash out CH_4, while reduction of the rains during April enhances the concentration of CH_4. From May, vegetation starts to dry, and at the same time, farmers harvest the crops. During this period, farmers burn crop residues coupled with changes in atmospheric circulation that allows the accumulation, hence increase CH_4 concentration levels. The pattern observed coincides with fire hotspots (Fig. S1), which gradually increases during the dry season over the study domain. A decrease in CH_4 between June and July has been explained in section 4.1. This indicates that land management, particularly regarding vegetation cover coupled with changes in weather patterns, significantly contributes to the concentration of CH_4 in the troposphere over the study domain. The rapid decrease of CO_2 during April and increase in the later months in the mid-troposphere is observed to have been affected by changes in air mass pattern (section 4.7) rather than vegetation only.

4.5. Implications with atmospheric water vapor

It is observed that the two trace gases, particularly, CH_4 concentration decrease with the increase of water vapor in the atmosphere (Fig. S4). This is because, with an increase in water vapor, more OH radicals are expected to be available to react with CH_4 (see Eqs. (2)–(4)), resulting in a rapid decrease of CH_4 from October throughout the wet months. The inverse happens during the dry months when low OH radicals are expected; however, except during the June–July season, probably some OH radicals produce (discussed in section 4.1) that suppress CH_4 concentration.

4.6. Climate response by CO_2 and CH_4 concentration

Changes in CO_2 and CH_4 concentration have a substantial impact on climate patterns through perturbating energy flow into and out of the climate system (IPCC, 2014). This occurs due to the absorption of longwave radiation by the two gases, which results in the distortion of shortwave and longwave radiative equilibrium. To restore the equilibrium, the climate system adjusts the temperature, also known as positive feedback, which results in external radiative forcing (RF) that restores radiative equilibrium (Etminan et al., 2016; Hofmann et al., 2006; Ramaswamy et al., 2019). An adjusted temperature associated with changes in CO_2 and CH_4 concentration in the radiative equilibrium is a fundamental key in the climate system as both gases contribute a high percentage of the total RF (IPCC, 2014). In the present study, therefore, the long-term (1985–2015) trend pattern of temperature was assessed and compared with the two trace gases in the last decade over the selected site using daily temperature observed at Chichiri meteorological station (Fig. 8). The long-term temperature trends revealed a general rise in temperature over Chichiri meteorological stations in the past three decades. A significant temperature change was observed in 2003. Temperature trends were further compared with those of trace gases (Fig. 8b–c) during the last decade (2004–2015). It can clearly be observed that both temperature and trace gases are increasing over the study domain. Interestingly, there is a steady increase in temperature from 2009 onwards, which coincides with the change point for the two

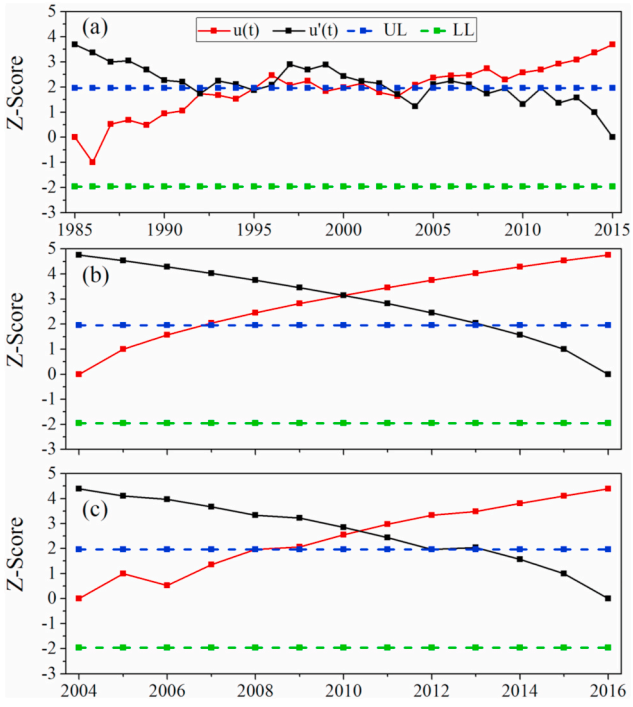

Fig. 8. Abrupt change of (a) temperature during 1985–2015, (b) CO_2 and (c) CH_4 during 2004–2016 derived from Sequential Mann-Kendal test statistic.

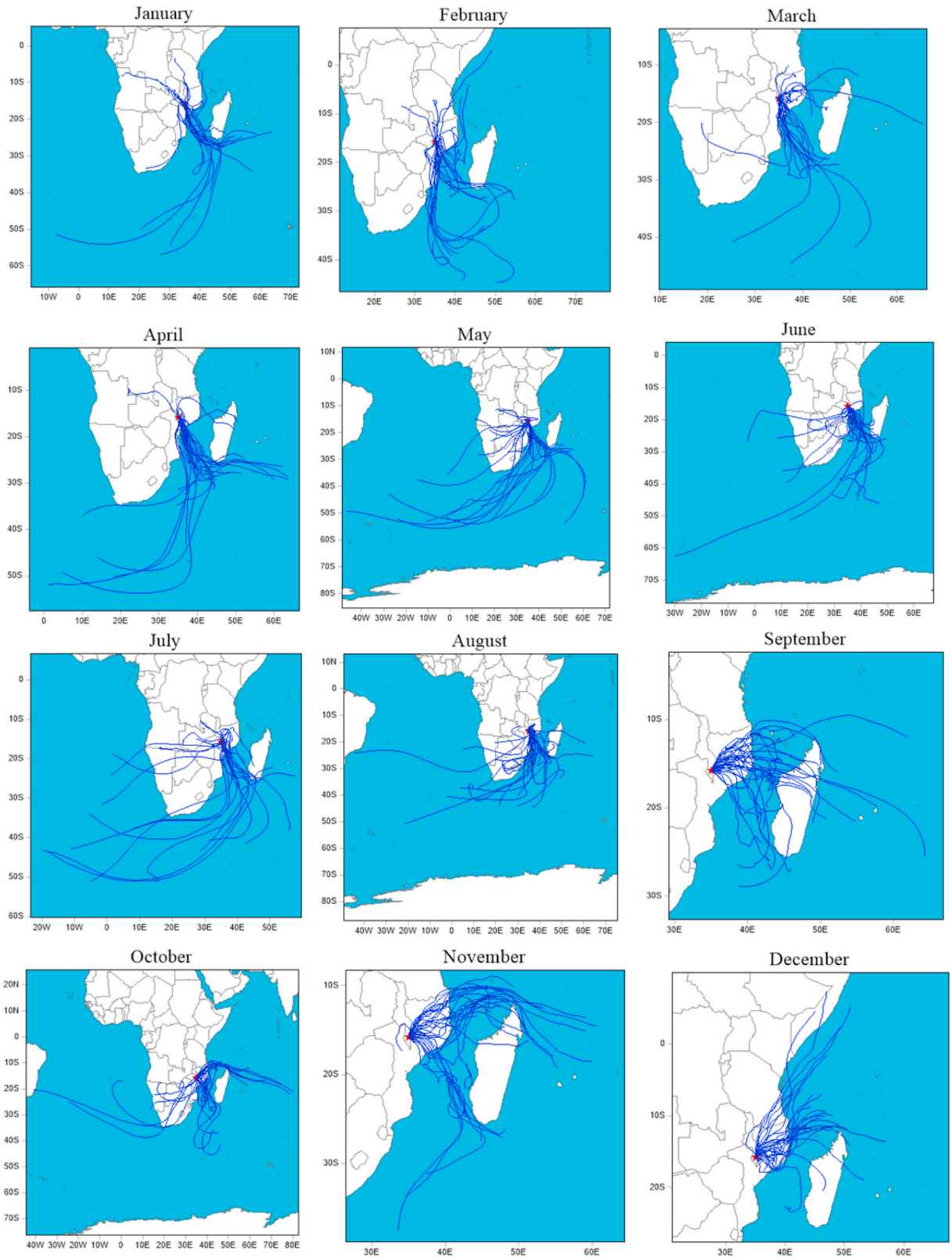

Fig. 9. 5-Day backward air mass trajectories ending over the selected site above 500 m ground level during each month of the year in 2016.

trace gases (Fig. 8b–c). A steady increase in temperature in the last decade signifies a temperature response to the significant rising of trace gases during 2010–2015.

It is worthy to note that positive feedback of temperature with the changes of CO_2 and CH_4 has a fundamental impact on climate systems, such as disruption of precipitation patterns due to excess heating. This resulted in adverse effects on agriculture systems due to high evaporation, which is highly sensitive to weather and climate variables over Sub-Sahara African regions, including Malawi (Kotir, 2011). The scatter plots between the temperature and trace gases (Fig. S6) revealed an

interesting pattern with a significant positive correlation when the concentration of these two trace gases was observed high (in SON season). The strong Pearson correlation coefficients were observed between temperature and CO_2 ($r = 0.75$, $p < 0.01$) and CH_4 ($r = 0.80$, $p < 0.01$) at 95% and 99% significant level during SON season when trace gases along with other pollutants concentrations are high. The above findings imply that the concentration of CO_2 and CH_4 during the SON season might have a significant influence on the temperature pattern over the selected site.

CO_2 and CH_4 were further compared with cloud optical properties, namely cloud fraction (CF) and cloud top temperature (CTT), to understand whether trace gases have any influence on them or not. The results show that CO_2 and CH_4 were positively correlated with CTT, such as ($r = 0.56$, $p < 0.05$) and ($r = 0.74$, $p < 0.01$), respectively, during the dry season (SON) (Fig. S6). It is of interest to note that excluding the outlier as shown in Fig. S6, CTT showed stronger correlations with CO_2 ($r = 0.73$, $p < 0.01$) and CH_4 ($r = 0.82$, $p < 0.01$). In contrast, CF exhibited profound negative correlation with CO_2 ($r = -0.54$, $p < 0.05$) and CH_4 ($r = -0.69$, $p < 0.01$) during the earlier season (SON) where pollution levels were high. It is also notable from Fig. S6 that the correlations of CO_2 and CH_4 with cloud properties were observed to be significant at a 95% significant level during SON season. High concentrations of CO_2 and CH_4 during SON season might have influenced cloud characteristics by modifying temperature patterns in the troposphere. Correlation coefficients of trace gases with temperature and cloud properties for the other seasons were generally insignificant (Table S1).

4.7. Influence of air masses

The analysis of air mass trajectories has recently been preferred to understand the long-range transport of pollutants from one place to another (Adesina et al., 2015; Boiyo et al., 2017; Nyasulu et al., 2020). In the present study, The HYSPLIT revealed the origin of multiple backward trajectories of air mass from distant locations arriving at the site (Fig. 9). The most dominant air masses; however, are observed to originate from the South Indian Ocean. During August and September, it is observed that air mass can travel from the South Atlantic Ocean through South Africa up to the selected site. Such air mass can transport carbon-containing pollutants from the South American continent and polluted areas of South Africa up to the study site and surrounding region. The air mass from the South American continent passing through South Africa has a significant contribution to the concentration of CO_2 observed in Fig. 3 during the June–August months. Similar results have been recently documented by Ncipha et al. (2020), who observed intercontinental transport of pollutants, mainly originating from the South American continent, which reaches different environments over South Africa. This is also in total agreement with the intercontinental movement of air mass and its contribution to the increase of pollutants, initiated by changes in atmospheric circulation over Southern Africa. From the previous studies (Edwards et al., 2006; Freitas et al., 2005; Reboita et al., 2010; Romatschke and Houze, 2010), it is observed that the air mass reaching the southern African continent in the troposphere is initiated by the anticyclonic circulation of the South Atlantic Ocean. The studies showed that the air mass from northern parts of the South American continent turns southwards on the western edge of the Atlantic anticyclone and crosses over the landmass of the South American continent. This air mass from South America then crosses over the South Atlantic Ocean, transporting pollutants from areas of active biomass burning that ends up in Southern Africa. This is consistent with the seasonal cluster analysis (Fig. S7), while 33% of air mass was captured extending further to the South Atlantic Ocean through South Africa during JJA. On the other way, the air mass originated from the South Indian Ocean during JJA, carries moisture, which reduces CH_4 by supplying more OH radicals that react with CH_4, which is evident from sections 4.1 and 4.5. Interestingly, the CO_2 is not affected by the influx of southeasterly moisture as compared to CH_4. This is because CO_2 is mostly influenced by westerlies from the South American continent in the mid-troposphere than CH_4, which is sourced from within the region, hence washed out in the lower troposphere by the moist south easterlies. During September to October months, the easterly air mass is the most dominant, which also coincides with easterly airflow (Fig. S2). It can be observed that easterly and southeasterly air mass traveled a short distance as compared to the air mass originating from the South Atlantic Ocean. This implies that the air mass spent much of the time over the land hence spreading regional pollutants such as from neighboring Mozambique, increasing trace gases, particularly CH_4, which is emitted within the region. Easterly air mass that extends further to Madagascar Islands transport pollutants from the islands; similar observation has been recently documented by Adesina et al. (2015) and Nyasulu et al. (2020). It is also of interest to note from the above results that a decrease in air mass contribution from South Atlantic Ocean through South Africa during SON was associated with a decrease of CO_2 as compared to JJA season, when high air parcel over the South Africa was associated with a high concentration of CO_2 in the troposphere.

As the peak of rainfall season approaches from December to February, the pattern of air mass change with a clear convergence system lies over the study domain. Air masses from Northwest (Congo), Southeast, and Northeast air mass all converge over the selected site. The most dominant air mass during DJF as observed in Fig. S7 is southeasterly (36%) and northeasterly (38%). The convergency system over the domain is also known as the Intertropical Convergence System (ITCZ) (Jury and Mwafulirwa, 2002). The convergency system brings pollutants from a region of active biomass burning such as Congo (de Graaf et al., 2010; Boiyo et al., 2017), which mixes with the locally produced pollutants though the concentrations of the pollutants are relatively low due to washout by excess rainfall. The Northeast air mass originates from the polluted region of the Middle East (Nyasulu et al., 2020), which transports pollutants; hence an increase in CO_2 observed during December. Lastly, March to May is dominated by air mass from the South Indian Ocean with fewer pollutants compared to the other months. This is also reflected in Fig. S3, where CO_2 is observed lowest in MAM season as it is mostly influenced by changes in air mass patterns.

5. Summary and conclusions

The long-term tropospheric CO_2 and CH_4 retrieved during 2004–2016 were analyzed from the AIRS sensor over the urban location of Malawi, Southeast Africa. The monthly variations showed an increase of CO_2 and CH_4 levels during the dry months from May to November, although CO_2 was found to exhibit another peak in December. CO_2 showed two peaks during July and December, while the highest peak for CH_4 was observed in September. The monthly variation of the two trace gases is highly associated with changes in precipitation, land cover, and anthropogenic activities, notably biomass burning coupled with vehicular and industrial emissions. Seasonal averages for CO_2 were recorded highest during JJA (388 ppm) and SON (388 ppm), while CH_4 had the highest records during SON (1823 ppb). The interannual characteristics revealed an increase in tropospheric CO_2 and CH_4 between 2004 and 2016 by 7.08% and 1.66%, respectively, during JJA and SON seasons, being the major contributors as they fall in the active biomass burning season over the region. Both the trace gases are highly correlated with carbon-containing compounds from incomplete combustion, suggesting the sources are from biomass burning, vehicle, and industrial emissions. The air mass backward trajectories demonstrated that pollutants by long-range atmospheric transport from active biomass burning region and local emissions could enhance concentration levels of CO_2 and CH_4. The main sinks of the two gases are occurred by precipitation and vegetation during the wet season over the study site.

CO_2 and CH_4 showed significant positive correlations with ambient temperature during the SON season. While temperature and trace gases, both levels were high, indicating a large warming effect and indirectly have a substantial influence on radiative forcing by the trace gases. We

also observed profound correlations between trace gases and cloud properties during which high pollution levels are noted over the sampling site. These findings demonstrated that trace gases have a large climatic effect in the Southeast Africa region. Therefore, the study recommends consistent monitoring of trace gases and assesses their climatic impact. Further, proper measures need to be considered that inhibit pollutants emissions strictly observed both at local and regional scales. This can heavily control the tropospheric concentration of CO_2 and CH_4 over the site and the entire region.

Credit author statement

Matthews Nyasulu: Formal analysis and Writing – original draft. Kanike Raghavendra Kumar: Reviewing and Editing. Noel Banda: Formal analysis. Brian Ayugi: Formal Analysis and Editing. Md. Jalal Uddin: Formal analysis. Md. Mozammel Haque: Supervision.

Declaration of competing interest

We all authors declare that we have no conflict of interest.

Acknowledgments

The scientific teams of NASA's AIRS and MODIS sensors are appreciated for making the datasets available online used in the present study. We are also grateful to the NOAA ARL for backward computing trajectories through the HYSPLIT model and the Department of Climate change and Meteorological Services (DCCMS), Malawi, for providing the meteorological data. The lead author (MN) would like to acknowledge the support offered by the Chinese Government through the China Scholarship Council (CSC). Also, the Nanjing University of Information Science and Technology (NUIST) and the Malawi Government through the Department of Climate Change and Meteorological Services recognized for the enormous support to pursue higher studies. One of the authors, KRK, is acknowledged to the Department of Science and Technology (DST), Govt. Of India, for the award of the DST-FIST Level-1 (SR/FST/PS-1/2018/35) scheme to the Department of Physics, KLEF, and also thankful to the Science and Engineering Research Board (SERB) of the DST for the sponsored research project under the Start-Up Research Grant (SRG) (File No. SRG/2020/001445).

Appendix A. Supplementary data

Supplementary data to this article can be found online at https://doi.org/10.1016/j.apr.2021.02.005.

References

Abed, F.G., Al-Salihi, A.M., Rajab, J.M., 2017. Space-borne observation of methane from atmospheric infrared sounder: data analysis and distribution over Iraq. J.of Appl. Adv. Res. 2 (4) https://doi.org/10.21839/jaar.2017.v2i4.100.

Adesina, A.J., Kumar, K.R., Sivakumar, V., 2015. Variability in aerosol optical properties and radiative forcing over Gorongosa (18.97oS, 34.35oE) in Mozambique. Meteorol. Atmos. Phys. 127 (2), 15. https://doi.org/10.1007/s00703-014-0352-2.

Alexander, F., 2017. Diagnosis of Floods/drought and Their Associated Circulation Anomaly over Malawi. Nanjing University of Information Science and Technology, Graduation thesis, pp. 1–35.

Ayugi, B.O., Tan, G., Ongoma, V., Mafuru, K.B., 2018. Circulations associated with variations in boreal spring rainfall over Kenya. Earth Syst Environ 2, 421–434. https://doi.org/10.1007/s41748-018-0074-6.

Baek, K.H., Kim, J.H., Park, R.J., Chance, K., Kurosu, T.P., 2014. Validation of OMI HCHO data and its analysis over Asia. Sci. Total Environ. 490, 93–105. https://doi.org/10.1016/j.scitotenv.2014.04.108.

Bai, W.G., Zhang, X.Y., Zhang, P., 2010. Temporal and spatial distribution of tropospheric CO2 over China based on satellite observations. Atmos.Sci 55 (31), 3612–3618. https://doi.org/10.1007/s11434-010-4182-4.

Billett, M.F., Harvey, F.H., 2013. Measurements of CO2 and CH4 evasion from UK peatland headwater streams. Biogeochemistry 114 (1–3), 165–181. https://doi.org/10.1007/s10533-012-9798-9.

Boiyo, R., Kumar, K. R., Zhao, T., and Bao, Y. (n.d.). Climatological analysis of aerosol optical properties over East Africa observed from space-borne sensors during 2001–2015. Atmos. Environ., 152, 298–313. https://doi.org/10.1016/j.atmosenv.2016.12.050.

Brunke, E., Labuschagne, C., Scheel, H., 2009. Long-term measurements of CO2 , CH4 , CO and O3 at cape point , South Africa. Geophys. Res 11 (October 2006), 3746.

Burney, J., Ramanathan, V., 2014. Recent climate and air pollution impacts on indian agriculture. Proc. Natl. Acad. Sci. Unit. States Am. 111 (46), 16319–16324. https://doi.org/10.1073/pnas.1317275111.

Cao, L., Chen, X., Zhang, C., Kurban, A., Qian, J., Pan, T., et al., 2019. The global spatiotemporal distribution of the mid-tropospheric CO 2 concentration and analysis of the controlling factors. Rem. Sens. 11 (1) https://doi.org/10.3390/rs11010094.

Chahine, M., Barnet, C., Olsen, E.T., Chen, L., Maddy, E., 2005. On the determination of atmospheric minor gases by the method of vanishing partial derivatives with application to CO2. Geophys. Res. Lett. 32 (22), 1–5. https://doi.org/10.1029/2005GL024165.

Chahine, M.T., Chen, L., Dimotakis, P., Jiang, X., Li, Q., Olsen, E.T., Yung, Y.L., 2008. Satellite remote sounding of mid-tropospheric CO2. Geophys. Res. Lett. 35 (17), 1–5. https://doi.org/10.1029/2008GL035022.

Chatterjee, S., Bisai, D., Khan, A., 2014. Detection of approximate potential trend turning points in temperature time series (1941-2010) for asansol weather observation station, West Bengal, India. Clim.Atmos.Sci 64–69. https://doi.org/10.4236/acs.2014.41009, 04(01).

Crutzen, P.J., Andreae, M.O., 1990. Biomass burning in the tropics: impact on atmospheric chemistry and biogeochemical cycles. Science 250 (4988), 1669–1678. https://doi.org/10.1126/science.250.4988.1669.

de Graaf, M., Tilstra, L.G., Aben, I., Stammes, P., 2010. Satellite observations of the seasonal cycles of absorbing aerosols in Africa related to the monsoon rainfall , 1995 e 2008. Atmos.Enviro. 44 (10), 1274–1283. https://doi.org/10.1016/j.atmosenv.2009.12.038.

Deltedesco, E., Keiblinger, K.M., Naynar, M., Piepho, H.P., Gorfer, M., Herndl, M., et al., 2019. Trace gas fluxes from managed grassland soil subject to multifactorial climate change manipulation. Appl. Soil Ecol. 137 (October 2018), 1–11. https://doi.org/10.1016/j.apsoil.2018.12.023.

Draxler, R., Hess, G., 1997. Description of the Hysplit_4 modelling system. In: NOAATech.Memo. ERL ARL 224, Air Resource Laboratory, Silver Spring,Md., Available. http://www.arl.noaa.gov/documents/reports/arl-224.pdf.

Edwards, D.P., Emmons, L.K., Gille, J.C., Chu, A., Attié, J.L., Giglio, L., et al., 2006. Satellite-observed pollution from Southern Hemisphere biomass burning. J. Geophys. Res. Atmos. 111 (14), 1–17. https://doi.org/10.1029/2005JD006655.

Eisele, F.L., Mount, G.H., Tanner, D., Jefferson, A., Shetter, R., Harder, J.W., Williams, E. J., 1997. Understanding the production and interconversion of the hydroxyl radical during the tropospheric OH photochemistry experiment. J. Geophys. Res. Atmos. 102 (5), 6457–6465. https://doi.org/10.1029/96jd02207.

Engelen, R.J., Serrar, S., Chevallier, F., 2009. Four-dimensional data assimilation of atmospheric CO2 using AIRS observations. J. Geophys. Res. Atmos. 114 (3), 1–12. https://doi.org/10.1029/2008JD010739.

Etminan, M., Myhre, G., Highwood, E.J., Shine, K.P., 2016. Radiative forcing of carbon dioxide, methane, and nitrous oxide: a significant revision of the methane radiative forcing. Geophys. Res. Lett. 43 (24) https://doi.org/10.1002/2016GL071930, 12,614-12,623.

Fiwa, L., Raes, D., 2014. Effect of rainfall variability on the length of crop growing period over the past three decades in central Malawi Effect of rainfall variability on the length of crop growing period over the past three decades in central Malawi. Clim. Res. https://doi.org/10.3354/cr01263 (January 2015).

Freitas, S.R., Longo, K.M., Silva Dias, M.A.F., Silva Dias, P.L., Chatfield, R., Prins, E., et al., 2005. Monitoring the transport of biomass burning emissions in South America. Environ. Fluid Mech. 5 (1–2), 135–167. https://doi.org/10.1007/s10652-005-0243-7.

Hansen, J., Sato, M., Kharecha, P., Russell, G., Lea, D.W., Siddall, M., 2007. Climate change and trace gases. Phil. Trans. Math. Phys. Eng. Sci. 365 (1856), 1925–1954. https://doi.org/10.1098/rsta.2007.2052.

Hofmann, D.J., Butler, J.H., Dlugokencky, E.J., Elkins, J.W., Masarie, K., Montzka, S.A., Tans, P., 2006. The role of carbon dioxide in climate forcing from 1979 to 2004: introduction of the annual greenhouse gas index. Tellus Ser. B Chem. Phys. Meteorol. 58 (5), 614–619. https://doi.org/10.1111/j.1600-0889.2006.00201.x.

IPCC, 2014. Climate change 2014 synthesis report summary Change. policymakers. Intergovernmental Panel on Climate Change. Available at:%0A/syr/AR5_SYR_FINAL_SPM.pdf. https://www.ipcc.ch/pdf/assessment-report/ar5.

Jury, M.R., Mwafulirwa, N.D., 2002. Climate variability in Malawi , Part 1 : dry summers , statistical associations and predictability. Int. J. Climatol. 1302, 1289–1302. https://doi.org/10.1002/joc.771.

Kahn, B.H., Irion, F.W., Dang, V.T., Manning, E.M., Nasiri, S.L., Naud, C.M., Worden, J. R., 2014. The atmospheric infrared sounder version 6 cloud products. Atmos. Chem. Phys. 14 (1), 399–426. https://doi.org/10.5194/acp-14-399-2014.

Kalanda-joshua, M., Ngongondo, C., Monjerezi, M., Liwenga, E.T., 2016. Climate Change in Semi-arid Malawi : Perceptions , Adaptation Strategies and Water Governance. https://doi.org/10.4102/jamba.v8i3.255 (January 2017).

Keeling, C.D., Bacastow, R.B., Bainbridge, A.E., 1976. Atmospheric carbon dioxide variations at mauna loa observatory, Hawaii. Tellus 28 (6), 538–551. https://doi.org/10.3402/tellusa.v28i6.11322.

Kendall, M.G., 1975. Rank Correlation Methods, fourth ed. Griffin, London, p. 202.

Kim, H.S., Chung, Y.S., Tans, P.P., Dlugokencky, E.J., 2015. Decadal trends of atmospheric methane in East Asia from 1991 to 2013. Air Qual, Atmos Health 8 (3), 293–298. https://doi.org/10.1007/s11869-015-0331-x.

Kirschke, S., Bousquet, P., Ciais, P., Saunois, M., Canadell, J.G., Dlugokencky, E.J., Zeng, G., 2013. Three decades of global methane sources and sinks. Nat. Geosci. 6 (10), 813–823. https://doi.org/10.1038/ngeo1955.

Kotir, J.H., 2011. Climate change and variability in Sub-Saharan Africa: a review of current and future trends and impacts on agriculture and food security. Environ. Dev. Sustain. 13 (3), 587–605. https://doi.org/10.1007/s10668-010-9278-0.

Kumbuyo, C.P., Yasuda, H., Kitamura, Y., Shimizu, K., 2014. Fluctuation of rainfall time series in Malawi : an analysis of selected areas. Geofizika 31. https://doi.org/10.15233/gfz.2014.31.1.

Lingaswamy, A.P., Arafath, S.M., Balakrishnaiah, G., Rama Gopal, K., Siva Kumar Reddy, N., Raja Obul Reddy, K., et al., 2017. Observations of trace gases, photolysis rate coefficients and model simulations over semi-arid region, India. Atmos. Environ. 158, 246–258. https://doi.org/10.1016/j.atmosenv.2017.03.048.

Machida, T., Matsueda, H., Sawa, Y., Nakagawa, Y., Hirotani, K., Kondo, N., Ogawa, T., 2008. Worldwide measurements of atmospheric CO2 and other trace gas species using commercial airlines. J.Atmos.Oce. Tech. 25 (10), 1744–1754. https://doi.org/10.1175/2008JTECHA1082.1.

Maddy, E.S., Barnet, C.D., Goldberg, M., Sweeney, C., Liu, X., 2008. CO2 retrievals from the atmospheric infrared sounder: methodology and validation. J. Geophys. Res. Atmos. 113 (11), 1–7. https://doi.org/10.1029/2007JD009402.

Mann, H.B., 1945. Nonparametric tests against trend. Econometrica 13, 245–259.

Mapoma, H.W.T., Tenthani, C., Tsakama, M., Kosamu, I.B.M., 2014. Air quality assessment of carbon monoxide, nitrogen dioxide and sulfur dioxide levels in Blantyre, Malawi: a statistical approach to a stationary environmental monitoring station. African J.Environ.Sci. Tech 8 (6), 330–343. https://doi.org/10.5897/ajest2014.1696.

Nakazawa, T., Sugawara, S., Inoue, G., Machida, T., Makshyutov, S., Mukai, H., 1997. Aircraft measurements of the concentrations of CO2, CH4, N2O, and CO and the carbon and oxygen isotopic ratios of CO2 in the troposphere over Russia. J. Geophys. Res. Atmos. 102 (3), 3843–3859. https://doi.org/10.1029/96jd03131.

Ncipha, X.G., Sivakumar, V., Malahlela, O.E., 2020. The influence of meteorology and air transport on CO2 atmospheric distribution over South Africa. Atmosphere 11 (3), 287. https://doi.org/10.3390/ATMOS11030287.

Ngongondo, C., Xu, C., Gottschalk, L., January 2014. Evaluation of spatial and temporal characteristics of rainfall in Malawi : a case of data scarce region. Theor. Appl. Climatol. 1–16. https://doi.org/10.1007/s00704-011-0413-0, 2011.

Nicholson, S.E., Klotter, D., Chavula, G., 2014. A detailed rainfall climatology for Malawi , Southern Africa. Int. J. Climatol. 325 (February 2013), 315–325. https://doi.org/10.1002/joc.3687.

Nyasulu, M., Haque, M.M., Boiyo, R., Kumar, K.R., Zhang, Y.L., 2020. Seasonal climatology and relationship between AOD and cloud properties inferred from the MODIS over Malawi, Southeast Africa. Atmos. Pollut. Rese. (July) https://doi.org/10.1016/j.apr.2020.07.023, 0–1.

Queface, A.J., Piketh, S.J., Annegarn, H.J., Holben, B.N., Uthui, R.J., 2003. Retrieval of aerosol optical thickness and size distribution from the CIMEL Sun photometer over Inhaca Island, Mozambique. J. Geophys. Res. Atmos. 108 (13) https://doi.org/10.1029/2002JD002374. SAF 45-1-SAF 45-9.

Rajab, J.M., Matjafri, M.Z., Lim, H.S., 2012. Methane interannual distribution over Peninsular Malaysia from atmospheric infrared sounder data: 2003-2009. Aerosol . Air. Qual. Res. 12 (6), 1459–1466. https://doi.org/10.4209/aaqr.2012.02.0039.

Ramanathan, V., Cicerone, R.J., Slngh, H.B., Kiehl, J.T., 1985. Climate Change, vol. 90, pp. 5547–5566.

Ramaswamy, V.R., Ollins, W.C., Aywood, J.H., Ean, J.L., Ahowald, N.M., Yhre, G.M., et al., 2019. Chapter 14 Radiative Forcing of Climate : the Historical Evolution of the Radiative Forcing Concept , the Forcing Agents and Their Quantification , and Applications, pp. 1–101. https://doi.org/10.1175/AMSMONOGRAPHS-D-19-0001.1.

Reboita, M.S., Nieto, R., Gimeno, L., Da Rocha, R.P., Ambrizzi, T., Garreaud, R., Krger, L. F., 2010. Climatological features of cutoff low systems in the Southern Hemisphere. J. Geophys. Res. Atmos. 115 (17), 1–15. https://doi.org/10.1029/2009JD013251.

Robles-Gonzalez, C., de Leeuw, G., 2008. Aerosol properties over the SAFARI-2000 area retrieved from ATSR-2. J. Geophys. Res. 113 (5), 1–10. https://doi.org/10.1029/2007JD008636.

Romatschke, U., Houze, R.A., 2010. Extreme summer convection in South America. J. Clim. 23 (14), 3761–3791. https://doi.org/10.1175/2010JCLI3465.1.

Saunois, M., Bousquet, P., Poulter, B., Peregon, A., Ciais, P., Canadell, J.G., Zhu, Q., 2016. The global methane budget 2000-2012. Earth Syst. Sci. Data 8 (2), 697–751. https://doi.org/10.5194/essd-8-697-2016.

Shi, Y., Matsunaga, T., Saito, M., Yamaguchi, Y., Chen, X., 2015. Comparison of global inventories of CO2 emissions from biomass burning during 2002-2011 derived from multiple satellite products. Environ. Pollut. 206, 479–487. https://doi.org/10.1016/j.envpol.2015.08.009.

Singh, R.B., Janmaijaya, M., Dhaka, S.K., Kumar, V., 2015. Study on the association of greenhouse gas (CO_2) with monsoon rainfall using AIRS and TRMM satellite observations. Phys. Chem. Earth 89 (90), 65–72. https://doi.org/10.1016/j.pce.2015.04.004.

Sneyers, R., 1990. On the statistical analysis of a series of observations. Tech Note 143, 192. WMO-No. 415.

Sparrevik, M., Utstøl, S., 2020. Assessing life cycle greenhouse gas emissions in the Norwegian defence sector for climate change mitigation. J. Clean. Prod. 248, 119196. https://doi.org/10.1016/j.jclepro.2019.119196.

Sreenivas, G., Mahesh, P., Subin, J., Lakshmi Kanchana, A., Venkata Narasimha Rao, P., Kumar Dadhwal, V., 2016a. Influence of meteorology and interrelationship with greenhouse gases (CO2 and CH4) at a suburban site of India. Atmos. Chem. Phys. 16 (6), 3953–3967. https://doi.org/10.5194/acp-16-3953-2016.

Sreenivas, K., Dadhwal, V.K., Kumar, S., Harsha, G.S., Mitran, T., Sujatha, G., Ravisankar, T., 2016b. Digital mapping of soil organic and inorganic carbon status in India. Geoderma 269, 160–173. https://doi.org/10.1016/j.geoderma.2016.02.002.

Strow, L.L., Hannon, S.E., 2008. A 4-year zonal climatology of lower tropospheric CO2 derived from ocean-only Atmospheric Infrared Sounder observations. J. Geophys. Res. Atmos. 113 (18), 1–20. https://doi.org/10.1029/2007JD009713.

Tans, P.P., Fung, I., Takahashi, T., 1990. 1990_TansFungTakahashi_etal.pdf.

Vakkari, V., Beukes, J.P., Dal Maso, M., Aurela, M., Josipovic, M., van Zyl, P.G., 2018. Major secondary aerosol formation in southern African open biomass burning plumes. Nat. Geosci. 11 (8), 580–583. https://doi.org/10.1038/s41561-018-0170-0.

Wagner, T., Beirle, S., Deutschmann, T., Eigemeier, E., Frankenberg, C., Grzegorski, M., Penning De Vries, M., 2008. Monitoring of atmospheric trace gases, clouds, aerosols and surface properties from UV/vis/NIR satellite instruments. J.Opt.A:PureAppl.Opt 10 (10). https://doi.org/10.1088/1464-4258/10/10/104019.

Wang, Y.Q., Zhang, X.Y., Draxler, R.R., 2010. TrajStat: GIS-based software that uses various trajectory statistical analysis methods to identify potential sources from long-term air pollution measurement data. Environ.Model. Softw 24 (8), 938–939. https://doi.org/10.1016/j.envsoft.2009.01.004.

Wei, C., Wang, M., Fu, Q., Dai, C., Huang, R., Bao, Q., 2020. Temporal characteristics of greenhouse gases (CO2 and CH4) in the megacity Shanghai, China: association with air pollutants and meteorological conditions. Atmos. Res. 235 (October 2019), 104759. https://doi.org/10.1016/j.atmosres.2019.104759.

WMO, 2019. WMO Statement on the Status of the Global Climate in 2013. WMO-No. 1130. Geneva, Switzerland. Retrieved from. https://drive.google.com/file/d/0BwdvoC9AeW-jUeEV1cnZ6Q URVaEE/edit?usp=sharing.

Xiong, X., Barnet, C., Maddy, E., Sweeney, C., Liu, X., Zhou, L., Goldberg, M., 2008. Characterization and validation of methane products from the atmospheric infrared sounder (AIRS). J. Geophys. Res. 113 (3), 1–14. https://doi.org/10.1029/2007JG000500.

Yadav, I.C., Linthoingambi Devi, N., Li, J., Syed, J.H., Zhang, G., Watanabe, H., 2017. Biomass burning in Indo-China peninsula and its impacts on regional air quality and global climate change-a review. Environ. Pollut. 227, 414–427. https://doi.org/10.1016/j.envpol.2017.04.085.

Zarenistanak, M., Dhorge, A.G., Kripalani, R.H., 2020. Trend analysis and change point detection of seasonal and annual precipitation in Iran. Int. J. Climatol. 40 (1), 308–323. https://doi.org/10.1002/joc.6211.